

Theoretical Solutions of Transient Spin Dynamics in Coherent SSFP

S-I. Urayama¹, L. Axel², J. Okamoto³, T. Azuma⁴, S. Tsutsumi⁵, N. Fukuyama¹

¹Human Brain Research Center, Kyoto University, Kyoto, Kyoto, Japan, ²Dept. Radiology, New York University, New York, NY, United States, ³MR Business Management Group, Siemens-Asahi Medical Technologies Ltd., Shinagawa-ku, Tokyo, Japan, ⁴Dept. Medical Simulation Engineering, Institute for Frontier Medical Sciences, Kyoto University, Kyoto, Kyoto, Japan, ⁵Dept. Medical Simulation Engineering, Institute for Frontier Medical Sciences, Kyoto University, Kyoto, Kyoto, Japan

Introduction Coherent SSFP imaging technique is being utilized for both anatomical and dynamic imaging applications, such as myocardial tagging or perfusion imaging. Therefore, many studies have been performed of theoretical and experimental analysis of transient spin dynamics in SSFP imaging. The transient response of the magnetization from the initial to the steady state is known to evolve along a spiral orbit in (M_x, M_y, M_z) coordinates; it can be obtained by calculating the eigenvalues and eigenvectors of a 3x3 matrix [1]. However, this matrix is too complex to solve analytically, so that solutions have not been previously presented. In this study, we show theoretical solutions of the eigenvalues and eigenvectors, by neglecting terms second order or higher in TR/T1 and TR/T2.

Theory According to [1], the 3x3 matrix \mathbf{T}_{SS} is given by eq.1, where $\mathbf{R}_n(\phi)$ is the ϕ -rotation matrix about the axis \mathbf{n} ($|\mathbf{n}|=1$), $\mathbf{n}_y = (0,1,0)$, $\mathbf{n}_z = (0,0,1)$, α is the flip angle, β is a precession angle during TR, and \mathbf{E} is a diagonal matrix whose diagonal components are (e_2, e_2, e_1) where $e_1 = \exp(-TR/T1)$ and $e_2 = \exp(-TR/T2)$, respectively. Two parameters θ and $\mathbf{a} = (a_x, a_y, a_z)$ are given by eq.2. Then, the orbit of the transient response just after the RF pulse is given by eq.3, where $\mathbf{m}(t)$ is the magnetization vector at time= t , \mathbf{m}_{SS} is the magnetization at the steady state, μ_i are the coefficients determined with the initial state, and λ_i, \mathbf{v}_i ($i=1,2,3$) are the i -th eigenvalues and eigenvectors of \mathbf{T}_{SS} , respectively. Theoretical analysis of the transient response is possible when \mathbf{m}_{SS} , λ_i and \mathbf{v}_i are solved analytically.

The resulting solutions are given by eq.4-6. The proof is omitted here because of the limited space. As shown in eq.4 and 6, two of three eigenvalues and eigenvectors are complex conjugate. Each eigenvector is the sum of a unit vector and a small orthogonal vector containing $(e_1 - e_2)$ and any pair of the unit vectors are also orthogonal. Then, the orbit during the transient time is given by eq.7, where ϕ_2 is the phase of λ_2 and $\mathbf{v}_{2r}, \mathbf{v}_{2i}$ are the real and imaginary components of \mathbf{v}_{2+} . Considering the eigenvector orthogonal relationships, the orbit is a spiral whose axis, rotating angle and shortening ratios in the axis and radial directions are $\mathbf{v}_1, \theta, \lambda_1$ and $|\lambda_2|$, respectively (Fig.1). Comparing \mathbf{m}_{SS} with \mathbf{v}_1 , the axis \mathbf{v}_1 is parallel to \mathbf{m}_{SS} if a_z is sufficiently larger than the coefficient of the second term in eq.5, but they are orthogonal if $a_z = 0$, i.e. $\beta = 0$. Since these equations are derived for a sequence with RF of only $+\alpha$ flip angle, those for the generally used sequence with RF of $\pm\alpha$ can be obtained by replacing β in eq.2-6 with $\beta + \pi$.

Validation Comparison between the numerically calculated values of $\lambda_i, \mathbf{m}_{SS}$ and \mathbf{v}_i from eq.4-6 and those from \mathbf{T}_{SS} are carried out under the conditions of $10^\circ \leq \alpha \leq 90^\circ$ (10° -step), $0^\circ \leq \beta \leq 360^\circ$ (10° -step), $2\text{msec} \leq TR \leq 5\text{msec}$ (1msec-step), $T1=250\text{msec}$ and $T2=50\text{msec}$. Since terms of the second order or higher in TR/T1 and TR/T2 are neglected in the approximation, T1 and T2 values of fat are selected as the shortest ones considered. Results shown in table.1 demonstrate the high accuracy obtained. In the presentation, we will present validation results with a phantom study which also demonstrates high coincidence with the solutions.

Conclusion Theoretical equations of the transient spin response in approaching SSFP are presented and the numerical validation demonstrates their high accuracy.

$$\mathbf{T}_{SS} \equiv \mathbf{R}_{\mathbf{n}_y}(\alpha)\mathbf{R}_{\mathbf{n}_z}(\beta)\mathbf{E} = \mathbf{R}_{\mathbf{a}}(\theta)\mathbf{E} \quad [1]$$

$$\begin{cases} \cos \theta = 2 \cos^2(\alpha/2) \cos^2(\beta/2) - 1 \\ \sin \theta = 2\kappa \cos(\alpha/2) \cos(\beta/2) \\ \mathbf{a} = \frac{1}{\kappa} \begin{pmatrix} \sin(\alpha/2) \sin(\beta/2) \\ \sin(\alpha/2) \cos(\beta/2) \\ \cos(\alpha/2) \sin(\beta/2) \end{pmatrix} \end{cases} \quad [2]$$

$$\left(\because \kappa = \sqrt{1 - \cos^2(\alpha/2) \cos^2(\beta/2)} \right)$$

$$\mathbf{m}(nTR) = \mathbf{m}_{SS} + \sum_{i=1}^3 \alpha_i \lambda_i^n \mathbf{v}_i \quad [3]$$

$$\begin{cases} \lambda_1 \equiv e_1 a_z^2 e_2^{1-a_z^2} = \exp\left\{-a_z^2 \frac{TR}{T1} - (1-a_z^2) \frac{TR}{T2}\right\} \\ \lambda_{2\pm} \equiv \begin{cases} -e_2, -e_1^{(1-a_z^2)} e_2^{a_z^2} = -\exp\left(-\frac{TR}{T2}\right), -\exp\left\{-\left(1-a_z^2\right) \frac{TR}{T1} - a_z^2 \frac{TR}{T2}\right\} & (\text{if } \beta \approx \pi) \\ e_1^{\frac{1-a_z^2}{2}} e_2^{\frac{1+a_z^2}{2}} e^{\pm i\theta} = \exp\left\{-\frac{1-a_z^2}{2} \frac{TR}{T1} - \frac{1+a_z^2}{2} \frac{TR}{T2}\right\} e^{\pm i\theta} & (\text{otherwise}) \end{cases} \end{cases} \quad [4]$$

$$\mathbf{m}_{SS} \equiv \frac{1-e_1}{1-\lambda_1} \left\{ a_z \mathbf{a} + \frac{(1-a_z^2)(1-e_2)}{2\sin(\alpha/2)} \begin{pmatrix} \cos(\alpha/2) \\ 0 \\ -\sin(\alpha/2) \end{pmatrix} \right\} \quad [5]$$

$$\begin{cases} \mathbf{v}_1 \equiv \mathbf{a} + \frac{a_z(1-a_z^2)(e_1-e_2)}{2\sin(\alpha/2)} \begin{pmatrix} \cos(\alpha/2) \\ 0 \\ -\sin(\alpha/2) \end{pmatrix} \\ \mathbf{v}_{2\pm} \equiv \frac{\sqrt{2}}{2} \left\{ \frac{1}{\kappa} \begin{pmatrix} -\sin^2(\alpha/2) \cos(\beta/2) \\ \sin(\beta/2) \\ -\sin(\alpha/2) \cos(\alpha/2) \cos(\beta/2) \end{pmatrix} + \frac{(1-a_z^2)(e_1-e_2) \cos \theta}{2\sin \theta} \begin{pmatrix} \cos(\alpha/2) \\ 0 \\ -\sin(\alpha/2) \end{pmatrix} \right\} \\ \pm i \frac{\sqrt{2}}{2} \left\{ \begin{pmatrix} \cos(\alpha/2) \\ 0 \\ -\sin(\alpha/2) \end{pmatrix} + \frac{(1-a_z^2)(e_1-e_2) \cos(\alpha/2)}{2\sin(\alpha/2)} \begin{pmatrix} \sin(\alpha/2) \\ 0 \\ \cos(\alpha/2) \end{pmatrix} \right\} \end{cases} \quad [6]$$

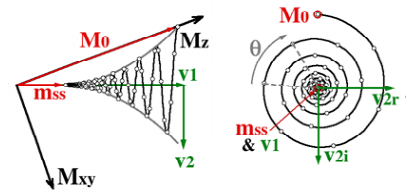


Fig.1 Spiral orbit and the vectors in lateral and frontal views. The envelope of the orbit satisfies $d_2 = d_1 \sqrt{\log(\lambda_2)/\log(\lambda_1)}$, where d_1 and d_2 are distance from \mathbf{m}_{SS} along \mathbf{v}_1 and \mathbf{v}_2 , respectively.

$$\mathbf{m}(nTR) - \mathbf{m}_{SS} = \mu_1 \lambda_1^n \mathbf{v}_1 + |\mu_{2+}| \lambda_{2+}^n \left\{ \cos(\phi_2 + n\theta) \mathbf{v}_{2r} - \sin(\phi_2 + n\theta) \mathbf{v}_{2i} \right\} \quad [7]$$

eqs. for error calc.	max.error	eqs. for error calc.	max.error
$ \lambda_{1T} - \lambda_{1N} /\lambda_{1N}$	0.11%	$ \mathbf{v}_{1T} - \mathbf{v}_{1N} $	0.03 Mo
$ \lambda_{2T} - \lambda_{2N} / \lambda_{2N} $	0.05%	$ \mathbf{v}_{2rT} - \mathbf{v}_{2rN} $	0.16 Mo
$ \arg(\lambda_{2T}) - \arg(\lambda_{2N}) $	0.26°	$ \mathbf{v}_{2iT} - \mathbf{v}_{2iN} $	0.07 Mo
$ \mathbf{m}_{SS T} - \mathbf{m}_{SS N} $	0.06 Mo		

table.1 Error validation results. The subscription T and N represent whose values/vectors are calculated from theoretical equations or numerical calculation from the matrix in eq.1, respectively. In all cases, the conditions of which the errors become maximum are $\alpha = 10^\circ$, $\beta = 0^\circ$ or 10° and $TR=5\text{msec}$.

[Reference] 1. MRM 46:149-158, 2001